Development of an Automatic Stencil Inspection System Using Modified Hough Transform and Fuzzy Logic

Kyung-Jin Choi, Young-Hyun Lee, Jong-Woo Moon, Chong-Kug Park, *Member, IEEE*, and Fumio Harashima, *Fellow, IEEE*

***Abstract*—In this paper, the authors present a system to inspect metal stencil that is used to print solder paste on pads of surface-mounted device on printed circuit board. The developed inspection system is composed of a moderately precise $X-Y$ robot and a vision system. To correct a position error caused by the $X-Y$ robot, the authors define position error vector and apply modified Hough transform to determine the dominant position error vector. Using this extracted dominant position error vector, the reference image is modified. This transformed reference image is compared with the camera image. Fuzzy logic is utilized to judge the correctness of the holes on the stencil. The input variables are the ratio of the overlapped area of two holes and the distance between the centroid of them. The output variable is the grade of the identity of the hole. These methods are verified by a simulation and applied to the inspection system.**

***Index Terms*—Automatic inspection system, fuzzy logic, modified Hough transformation (MHT), stencil (metal mask).**

I. Introduction

RECENTLY, there are many automatic equipment in surface mount technology (SMT) inline production systems, such as solder cream printer, chip mounter, and reflower. For the inspection of the errors in each process, cream solder print inspection system, chip mount inspection system, and solder inspection system are used.

The error rate of each process is investigated. The result shows that the error rate in solder cream printing process ranges from 64% to 70%. There are two reasons for this high error rate. One is that metal stencil has some defect. The other is that some holes are clogged by cream solder while printing. Therefore, the quality of metal stencil is very important for the following processes.

In this paper, we bring the first problem into focus. That is, we plan to develop a system to inspect the metal stencil. We composed the inspection system using a low-precision $X-Y$ robot and a vision system. To correct the position errors caused by the low-precision $X-Y$ robot, many control algorithms are proposed [1]–[7]. However, these methods are very complex, and they need the exact parameter estimation. Furthermore, they have some drawbacks for industrial application. A different approach was needed. We defined the position error vector and applied modified Hough transform (MHT). In addition, fuzzy logic was applied to decide whether the holes were correct. It is more flexible and humanlike.

This paper is organized as follows. In Section II, we give an explanation of metal stencil, the aim of the inspection, and the structure of the system. In Section III, the definition of the position error vector and that of the MHT are introduced. In Section IV, fuzzy logic for this application is also introduced. The simulation and experimental results are shown in Section V. Section VI concludes the paper.

II. Metal Stencil and Inspection System

A. Metal Stencil

Metal stencil is usually used to print solder cream on printed circuit board. The material is a thin stainless steel. The holes of the metal stencil have various shapes and sizes, such as polygons, circles, and quadrangles, and are cut by a laser machine according to a Gerber file. The format of the Gerber file is RS-274D/X and is used by a computer-aided design system. For the inspection, a reference image is needed. This image is created and drawn by this Gerber file. Fig. 1 is an example of metal stencil. The main function of our system is to detect the holes that are different from the reference holes.

B. Inspection Criteria

In case of an abrupt power change of the laser machine, the hole of the stencil is not made correctly. Such holes are defined as errors. To detect these errors, hole position and hole area are used. An error detection rule is generally as follows:

Rule 1: Center_Dist $= \sqrt{(x_1-x_2)^2+(y_1-y_2)^2} < T$

Rule 2: Area_Ratio $= |1.0 - S_1/S_2| < R.$

Here, (x_1, y_1) is the hole position in reference image, and S_1 is the area of the hole. (x_2, y_2) is the hole position closest to

Manuscript received November 30, 2004; revised December 8, 2005. Abstract published on the Internet on September 15, 2006.

K.-J. Choi and Y.-H. Lee are with the School of Electronics, Systems and Information Engineering, Kangnam University, Yongin 449-702, Korea (e-mail: kjchoi@kangnam.ac.kr; yhlee@kangnam.ac.kr).

J.-W. Moon is with the School of Digital Electronics, Busan College of Information Technology, Busan 616-737, Korea (e-mail: sucuba@bit.ac.kr).

C.-K. Park is with the School of Electronics and Information, Kyunghee University, Yongin 449-701, Korea (e-mail: ckpark@khu.ac.kr).

F. Harashima is with Tokyo Denki University, Tokyo 101-8457, Japan (e-mail: f.harashima@cck.dendai.ac.jp; president@dendai.ac.jp; f.harashima@ieee.org).

Digital Object Identifier 10.1109/TIE.2006.885494

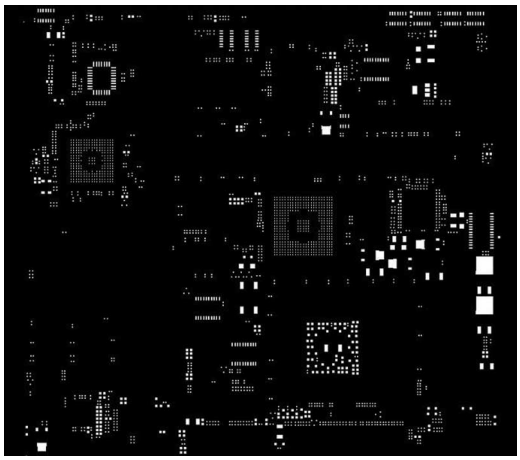

Fig. 1. Example of metal stencil.

TABLE I
RESULT OF JUDGMENT USING THE FIXED THRESHOLD VALUE

Area_Ratio	Center_Dist	Judgment
0.086826	10.052346	Error
0.072948	10.089727	Error
0.353183	5.3994381	Error

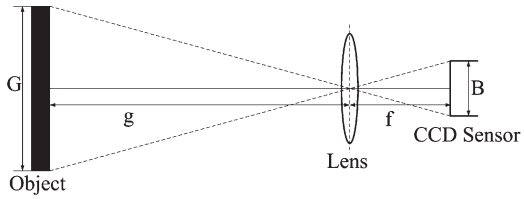

Fig. 2. Relationship between camera, lens, and object.

(x_1, y_1) in the camera image, and S_2 is the area of the hole. Rule 1 is the condition for the position difference of these two holes, which must be less than the threshold value T that is about 200 μm. This value corresponds to ten pixels if a camera resolution is 200 μm. Rule 2 is the condition for the existence of a hole. The value R is about 0.35 (65%). If the two conditions are satisfied, then a hole is correct.

However, if the fixed threshold value is used as above, some ambiguous judgment can be made. Some sample cases are shown in Table I. A human being would have judged them to be correct. To solve this problem, we used fuzzy logic.

C. Structure of Inspection System

The inspection system consists of the subsystems. One is a vision system. In the vision system, we use monochrome area scan camera (ASC) to obtain the real image. In case of using ASC, only one field of view (FOV) can be inspected at a time. It can be defined as Fig. 2 and

$$G \times f = g \times B \tag{1}$$

where G is the FOV, f is the focal length, g is the working distance, and B is a charge-coupled device cell. Therefore, the whole area of the metal stencil must be divided into several inspection blocks that are equal to FOV.

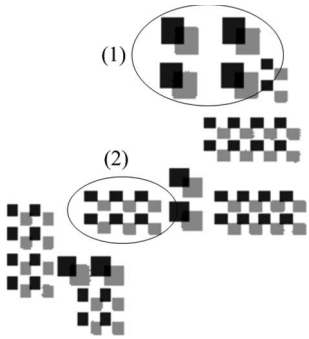

Fig. 3. Position error between two images.

The other subsystem is the $X - Y$ robot to move the vision system to the center of the next inspection block. The type of the motion system is a ball screw type, which has the accuracy of about ± 1.0 mm. This error is caused by the mechanical defects such as backlash, friction, and load inertia. Because of this, the camera cannot be positioned precisely enough. Therefore, the camera image cannot be matched with the reference image in Fig. 3. If we use dynamic equation to correct this error, it is very hard and complex to solve it. Furthermore, other mechanical errors can be included. We solve this problem as follows: The position error vector is defined to compensate these position errors, and the MHT method is applied on the basis of this vector.

III. INSPECTION ALGORITHM

The algorithm for compensating the position error in Fig. 3 seems to be similar with that for template matching or map matching [8]–[10]. However, there are some differences in a few points of view. First of all, which region would be selected for the calculation of position error within an image? If we select region (1) in Fig. 3, the process is very simple and easy. However, we have to define many complex criteria. If we select region (2) instead of region (1), we may easily calculate the position error. However, we may make a mistake in deciding the direction because the affiliation of each image cannot be easily determined. For the calculation of the position error, in this paper, we define position error vector and apply it to MHT. Fig. 4 describes the algorithm proposed to calculate and compensate the position error.

A. Image Processing

The camera image is transformed into a binary image using a threshold value. The information of each hole that exists in both images such as centroid, area, width, and height is calculated through a labeling. Among them, the centroid of a hole is calculated by

$$\mathrm{CX}_n = \frac{1}{m_i}\sum_{i\in n} x_i, \quad \mathrm{CY}_n = \frac{1}{m_i}\sum_{i\in n} y_i, \qquad n = 1, 2, \ldots, n \tag{2}$$

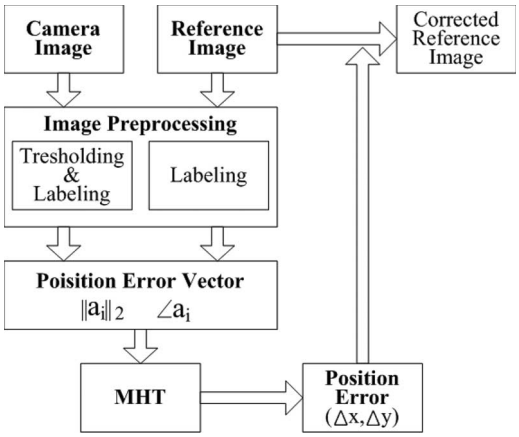

Fig. 4. Algorithm for calculating position error.

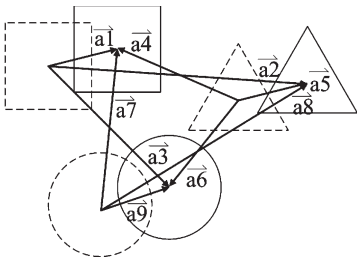

Fig. 5. Position error vectors.

where CX_n, CY_n is the centroid of a hole, n is the number that is given through a labeling, m_i is the number of the pixel of each hole, and x_i and y_i is the position of the pixel. The centroid of holes is used for the definition of the position error vector.

B. Definition of the Position Error Vector

Fig. 5 shows a position error between two images. The solid lines are the holes of the camera image, and the dotted lines are those of the reference image. The position error vector is defined as the vector between the centroid of the holes on a reference image and the centroid of the holes on a camera image.

C. MHT

The Hough transform (HT) is a well-known method to detect lines, circles, or other analytic curves of the points in complex and noisy images. In the HT, a voting process transforms the set of points in the image space into a set of accumulated votes in the parameter space. Therefore, the HT converts a difficult global detection problem in the image space into a more easily solved local peak detection problem in the parameter space. There are many applications, such as the detection of edge points [13]–[15], the calculation of orientation [11], [13], [14], or displacement [12], [13].

Ballard [16] further expands the HT to the recognition of the objects with arbitrary shapes, which is named the generalized HT (GHT). In the GHT, the parameter space is composed by

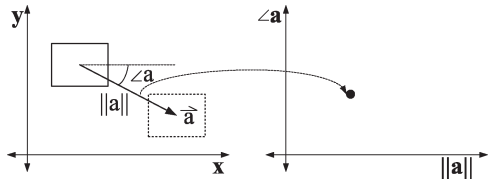

Fig. 6. Mapping into parameter space.

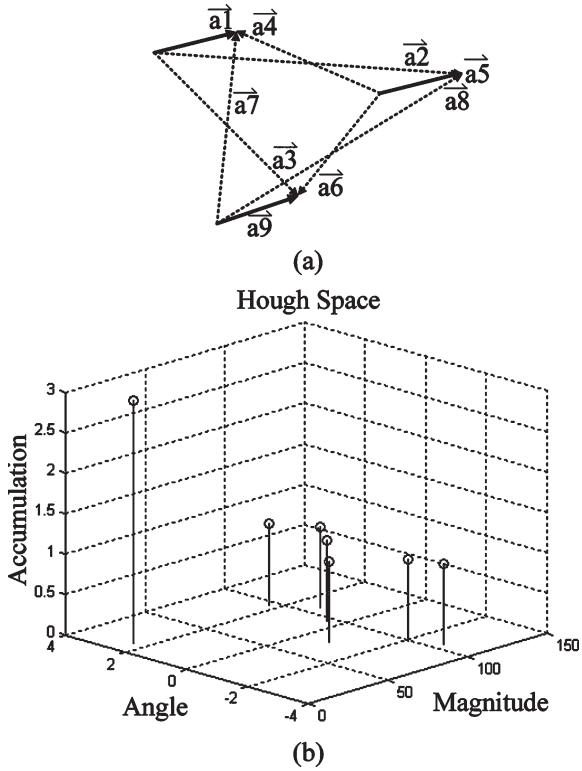

Fig. 7. (a) Extracted position error vector. (b) Parameter space.

the parameters that are arbitrarily selected according to the application. Tsai [13] selected the distance between the edge point and the arbitrary point, which is in the object and the vector that is formed by two points as the parameters. Wen and Lozzi [17] selected the scale factor for the variation of the object size and the angle as the parameter.

In this paper, we select the magnitude and the angle of the position error vector as the parameters. In Cartesian coordination, the position error vector has its magnitude and angle. The position error vector transforms a point in the parameter space as in Fig. 6.

We carry out the voting process for all of the position error vectors. As a result, we can select local peak bin in the parameter space and the position error vector in the Cartesian space in Fig. 7. We calculate the displacement Δx and Δy by

$$\Delta x = \|a_i\|_2 \cos(\angle a_i) \quad \Delta y = \|a_i\|_2 \sin(\angle a_i). \tag{3}$$

Then, the position of the reference image is modified by this displacement. Finally, the reference image is in a correct positional arrangement with the camera image.

TABLE II
INPUT VARIABLE 1

Linguistic Variable Name	Area_Ratio
Calculation	$\lvert 1.0 - S_1 / S_2 \rvert$
Dimension	0 < Area_Ratio < 1
Linguistic Terms	S(Small) : Two holes are similar in size.
	N(Normal) : Ambiguous
	L(Large) : Two holes are dissimilar in size

TABLE III
INPUT VARIABLE 2

Linguistic Variable Name	Center_Dist
Calculation	$\sqrt{(x_1 - x_2)^2 + (y_1 - y_2)^2}$
Dimension	0 < Center_Dist < 100
Linguistic Terms	S(Short) : Two holes are located nearby
	N(Normal) : Ambiguous
	L(Long) : Two holes are located far apart

TABLE IV
OUTPUT VARIABLE

Linguistic Variable Name	Judge_Ratio
Calculation	Center of Area
Dimension	0 < Judge_Ratio < 1
Linguistic Terms	E(Error)
	A(Ambiguous)
	C(Correct)

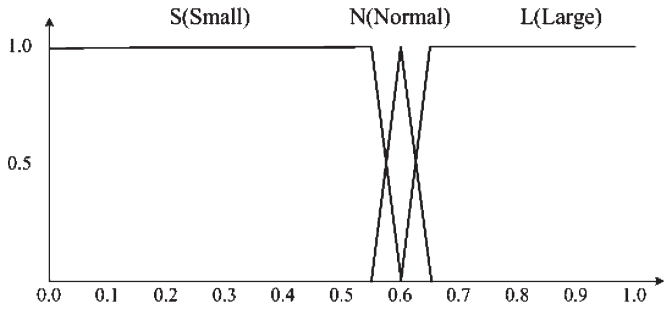

Fig. 8. Membership functions of the Area_Ratio.

D. Fuzzy Logic for Error Detection

In case of using a fixed threshold value to detect the error, there are some problems as described in Section II-B. To solve this problem and to make a more flexible judgment as a human expert makes, the fuzzy logic is used [18].

The fuzzy decision-making system has two input variables. One is the ratio of the area between two holes. The other is the center distance between them. The output variable of fuzzy system is the fuzzy decision for error existence. Tables II–IV show the information about the input and output variables in detail. The membership functions are shown in Figs. 8–10. The fuzzy rule base is defined in Table V.

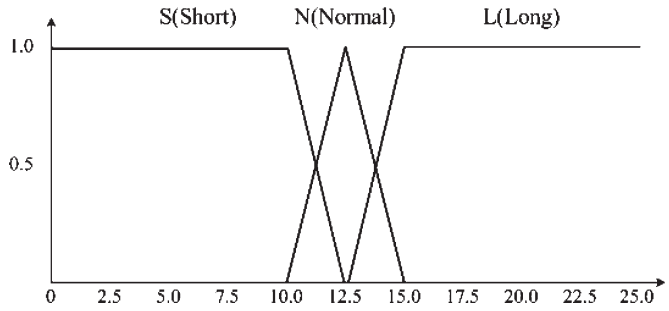

Fig. 9. Membership functions of the Center_Dist.

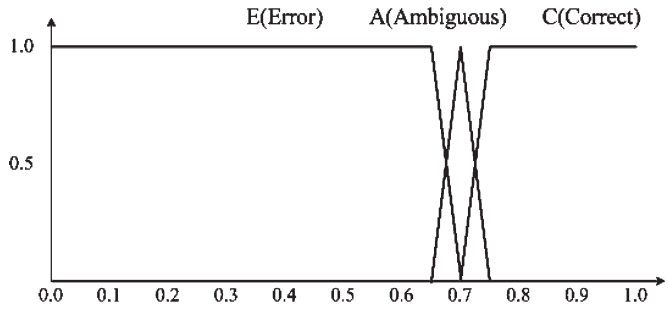

Fig. 10. Membership functions of the Judge_Ratio.

TABLE V
FUZZY RULE BASE

Center_Dist \ Area_Ratio	S (Small)	N (Normal)	L (Large)
S(Short)	C	C	E
N(Normal)	C	A	E
L(Long)	E	E	E

TABLE VI
COMPONENTS OF THE INSPECTION SYSTEM

Vision System	CCD Camera	Monochrome, 1300×1030, 2EA
	Lens	35 mm
	Graber Board	Metrox Meteor2-MC
	Illumination	Back-light Fluorescent Light
	FOV	25×20 (mm)
	Resolution	19.5×19.5 (μm)
X-Y Robot	Motor	Mitsubishi AC Servo Motor
	Controller	ADLINK PCI-8132
	Accuracy	± 1.0 (mm)

IV. EXPERIMENT

A. Components of Inspection System

The component of the inspection system is shown in Table VI. Fig. 11 shows the inspection system and the program graphic user interface.

B. Experimental Result

In Fig. 12, the result of the position error compensation about an inspection block is shown. Fig. 12(a) shows the position error. After the proposed algorithm had been applied, the error was exactly compensated as shown in Fig. 12(b). Fig. 12(c) is the parameter space, which shows the voting result. The dominant position error vector, which has a magnitude of

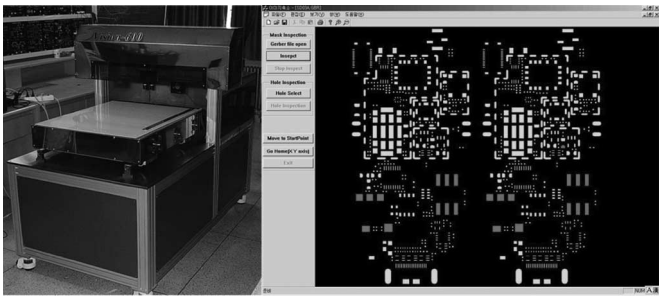

Fig. 11. Metal stencil inspection system and its graphic user interface.

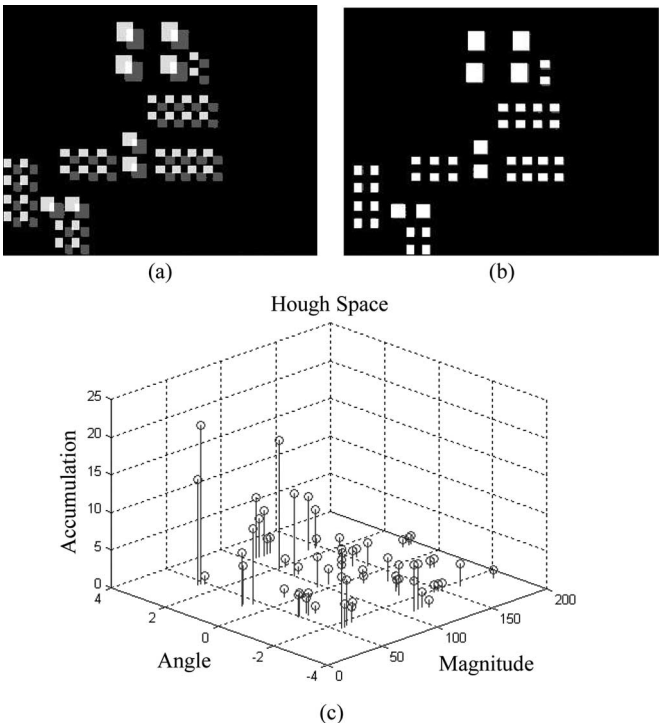

Fig. 12. Experimental results for position error. (a) Before error correction. (b) After error correction. (c) Parameter space.

46.33 and an angle of 2.57°, is calculated. From (3), the position error of the x-axis is -39 pixels, which is about 760.5 μm, and the position error of the y-axis is 25 pixels, which is about 487.5 μm. Also, the correlation coefficient is calculated to show the extent of collision of the two images. The correlation coefficient was 0.075 before the compensation, and after the compensation, it was improved up to 0.945. The correlation coefficient is calculated, and its dimension is from 0 to 1 [19], i.e.,

$$r = \frac{\sum \left[f_1(x,y) - \overline{f_1} \right] \left[f_2(x,y) - \overline{f_2} \right]}{\left\{ \sum f_1(x,y) - \overline{f_2}]^2 \sum f_2(x,y) - \overline{f_1}]^2 \right\}^{1/2}} \qquad (4)$$

where r is the correlation coefficient, $f_1(x,y)$ is the reference image, $f_2(x,y)$ is the camera image, and $\overline{f_1}$ and $\overline{f_2}$ are the average intensities of the images.

The correlation coefficients were calculated for all inspection blocks in four metal stencil samples, and the result is shown in Fig. 13. In Fig. 13, the rectangles indicate the correlation coefficients before the position error is corrected, whereas

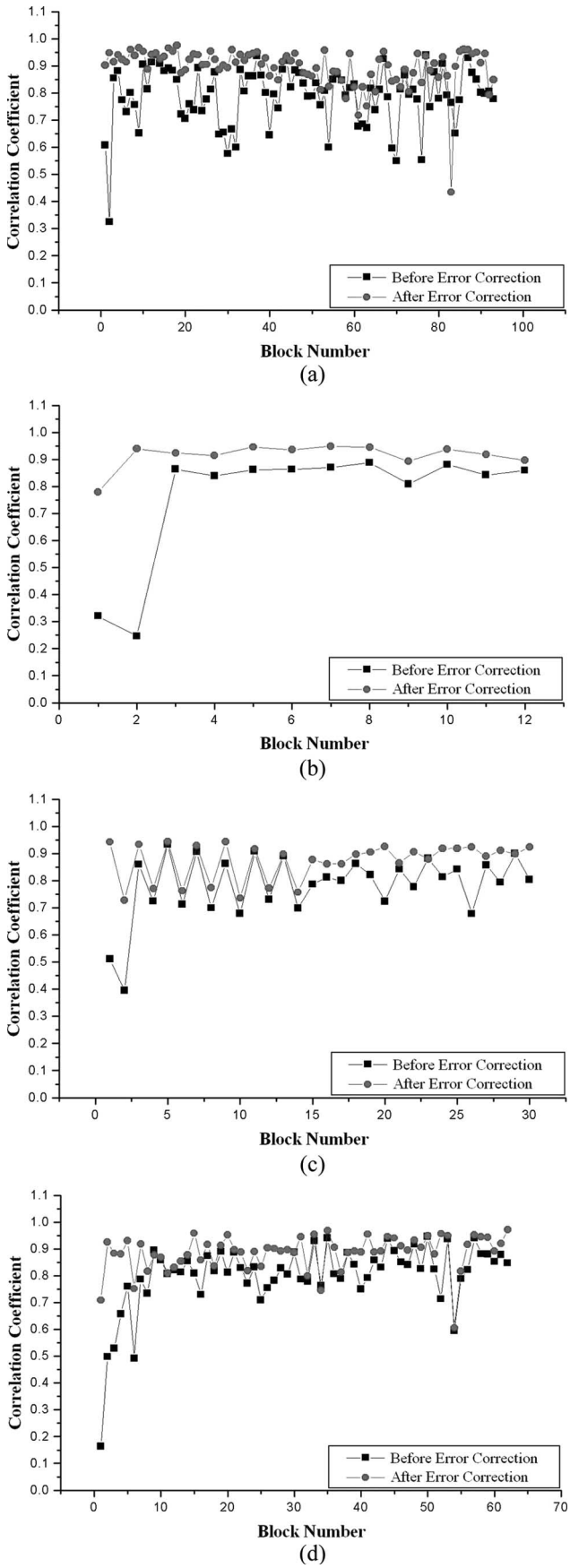

Fig. 13. Correlation coefficient of metal stencil samples. (a) Correlation coefficient of sample 1. (b) Correlation coefficient of sample 2. (c) Correlation coefficient of sample 3. (d) Correlation coefficient of sample 4.

TABLE VII
AVERAGE OF THE CORRELATION COEFFICIENT

	Before the compensation	After the compensation
Sample 1	0.79	0.90
Sample 2	0.76	0.92
Sample 3	0.78	0.87
Sample 4	0.80	0.89

the circles show the correlation coefficients after the position error is corrected. Table VII is the average of the correlation coefficient for each sample.

In accordance to the fuzzy rule in Section IV, the fuzzy decision space is shown in Fig. 14(a). The red region shows correct holes, whereas the blue one shows error. In addition, the middle region shows the decision by the fuzzy logic.

The fuzzy decision rules were applied to the sample metal stencil. The result is shown in Table VIII and Fig. 14(b)–(d). In Table VIII, fuzzy rules have no effect on judgment in sample 2. However, in samples 1, 3, and 4, the effect of the fuzzy decision system can be seen. Fig. 14(b)–(d) shows that the hole is correct in case that the two holes are very much similar in size, even if the distance between two holes is more than about two or three pixels (40–60 μm). That is not the case when using crisp value. Therefore, unnecessary error detection is reduced to about 48.5% by applying the fuzzy rule. The reason why this phenomenon generates is that steel film must be spanned when metal stencil is produced. Because of this tension, the position of the holes can be different from the position of the holes in Gerber file. Actually, sample 1 has 5596 holes, sample 2 has 1154 holes, sample 3 has 734 holes, and sample 4 has 1928 holes. In addition, the size of sample 1 is 240 $\times$ 240 mm; that of sample 2 is 90 $\times$ 94 mm; that of sample 3 is 160 $\times$ 210 mm; and that of sample 4 is 110 $\times$ 150 mm. Therefore, this tension can affect samples 1, 3, and 4 more than it can affect sample 2.

The result of this experiment on real errors detection is the same in Table IX. Two holes of sample 1 could not be detected because the size of the hole is bigger than FOV. An unexpected hole in sample 3 and two holes in sample 4 were detected because the holes were covered with dust. However, this error can be considered to be correct. Finally, we defined error detection rate (EDR) as (5), shown at the top of the next page. The average EDR in our experiments is 99.931%. It shows that the proposed fuzzy decision rule and the inspection algorithm are very efficient.

V. CONCLUSION

In this paper, inspection system for metal stencil is developed. Inspection system is composed of a low-precision $X - Y$ robot and a vision system. For our inspection system, two algorithms are proposed to be applied. To correct position error caused by a low-precision $X - Y$ robot, position error vector is defined. This position error vector is defined by the position of the objects that exist in reference image and camera image. The MHT is applied for the purpose of determining the dominant position error vector. The reference image is modified by the

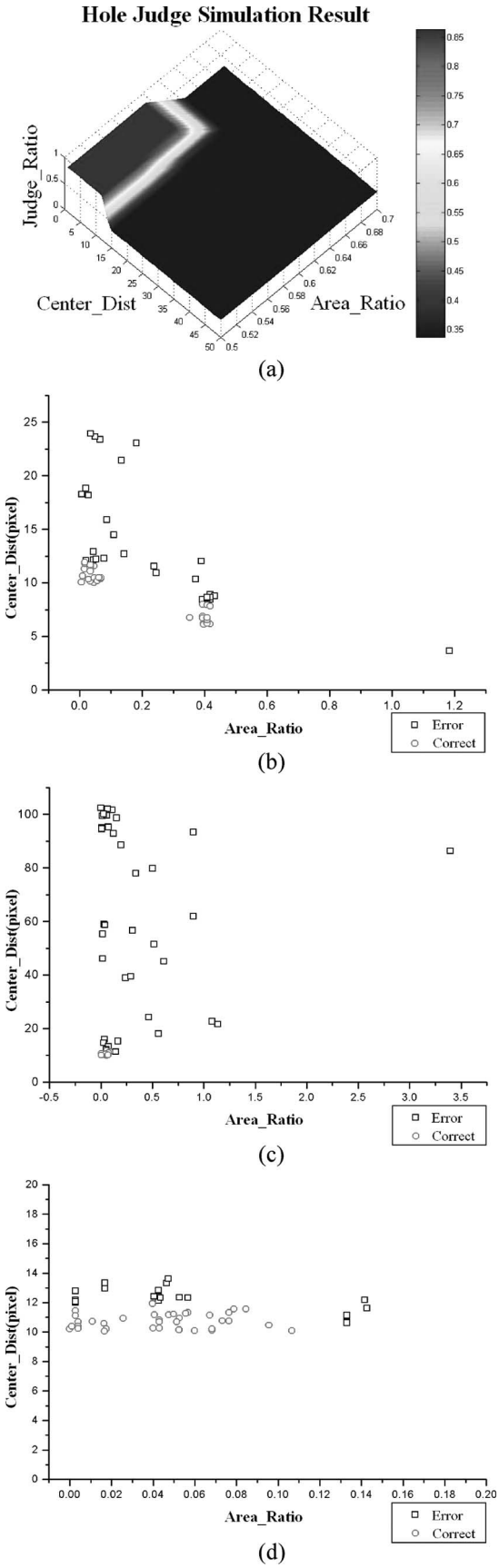

Fig. 14. Experimental result using fuzzy rule in samples. (a) Judgment region by fuzzy rule. (b) Experimental result using fuzzy rule in sample 1. (c) Experimental result using fuzzy rule in sample 3. (d) Experimental result using fuzzy rule in sample 4.

$$\text{Error Detection Rate} = \left(1 - \frac{|\text{Number of Substantial Error} - \text{Number of Detected Error}|}{\text{Total Number of Test Hole}}\right) \times 100(\%) \quad (5)$$

TABLE VIII
COMPARISON OF ERROR DETECTION

	Crisp Value used	Fuzzy Rule base	Improvement (%)
Sample 1	65	28	56.9
Sample 2	27	27	0
Sample 3	49	38	22.5
Sample 4	59	20	66.1

TABLE IX
ERROR DETECTION RESULTS

	Total Hole	Error Hole	Detected Error Hole	EDR(%)
Sample 1	5596	12	10	99.964
Sample 2	1154	22	22	100.0
Sample 3	734	10	11	99.864
Sample 4	1928	10	12	99.896

extracted dominant position error vector, and the new reference image is obtained. As a result of the experiment using four metal stencil samples, the average of correlation coefficient is 0.90. It represents that position error is compensated precisely. In addition, the fuzzy logic is used to judge if the holes are error or not. The input variables are the ratio of the area and the distance between the centroid of the holes. The output variable is the fuzzy decision for error existence. In comparison with the inspection criteria using crisp value, error detection ratio is reduced to about 48.5%. Therefore, we could make more flexible and humanlike judgment. The effectiveness and the performance of these methods are verified by a simulation and by applying to the inspection system.

If the algorithms proposed in this paper are applied, the exact parameter estimation on friction, load inertia, and backlash, as well as the complex control algorithms, are not anymore necessary to be regarded. Therefore, we can make a simple control algorithm and lower the system price. In addition, making a reference image from a Gerber file is applicable to most of the inspection systems in SMT inline systems.

REFERENCES

[1] W. Li and M. Rehani, "Modeling and control of a belt-drive positioning table," in *Proc. IEEE 22nd IECON*, 1996, vol. 3, pp. 1884–1989.

[2] W. Li and X. Cheng, "Adaptive high-precision control of positioning tables—Theory and experiments," *IEEE Trans. Control Syst. Technol.*, vol. 2, no. 3, pp. 265–270, Sep. 1994.

[3] Z. Zhao and L. Cai, "On the improvement of tracking performance of positioning tables," in *Proc. IEEE 22nd IECON*, 1996, vol. 3, pp. 1990–1995.

[4] K. Lim, J.-W. Seo, and C.-H. Choi, "Position control of XY table in CNC machining center with non-rigid ballscrew," in *Proc. Amer. Control Conf.*, 2000, pp. 1542–1546.

[5] G. Tao and P. V. Kokotovic, "Adaptive control of systems with unknown output backlash," *IEEE Trans. Autom. Control*, vol. 40, no. 2, pp. 326–330, Feb. 1995.

[6] K. T. Woo, W. Li-Xin, F. L. Lewis, and Z. X. Li, "A fuzzy system compensator for backlash," in *Proc. IEEE Int. Conf. Robot. Autom.*, 1998, pp. 181–186.

[7] T. Jukic and K. Peric, "Model based backlash compensation," in *Proc. Amer. Control Conf.*, 2001, pp. 775–780.

[8] H.-C. Liu and M. D. Srinath, "Partial shape classification using contour matching in distance transformation," *IEEE Trans. Pattern Anal. Mach. Intell.*, vol. 12, no. 11, pp. 1072–1079, Nov. 1990.

[9] M.-H. Han, D. Jang, and J. Forster, "Inspection of 2-D objects using pattern matching method," *Pattern Recognit.*, vol. 22, no. 5, pp. 567–574, 1989.

[10] G. Zhang, M. Jing, R. Hu, and Z. Chen, "A new image matching method based on principal component analysis," *Proc. SPIE*, vol. 4222, pp. 337–340, 2000.

[11] B.-J. You, Y. S. Oh, and Z. Bien, "A vision system for an automatic assembly machine of electronic components," *IEEE Trans. Ind. Electron.*, vol. 37, no. 5, pp. 349–357, Oct. 1990.

[12] L. Locchi, D. Mastrantuono, and D. Nardi, "A probabilistic approach to Hough localization," in *Proc. IEEE Int. Conf. Robot. Autom.*, May 2001, pp. 4250–4255.

[13] D.-M. Tsai, "An improved generalized Hough transform for the recognition overlapping objects," *Image Vis. Comput.*, vol. 15, no. 12, pp. 877–888, Dec. 1997.

[14] E. R. Davies, "Application of the generalized Hough transform to corner detection," *Proc. Inst. Electr. Eng.—Comput. Digit. Tech.*, vol. 135, no. 1, pt. E, pp. 49–54, Jan. 1988.

[15] E. P. Da Silva and A. Gonzaga, "Finding the position and area of an object in a visual inspection system," in *Proc. 2nd Workshop Cybernetic Vision*, 1997, pp. 93–98.

[16] D. H. Ballard, "Generalizing the Hough transform to detect arbitrary shape," *Pattern Recognit.*, vol. 13, no. 2, pp. 111–122, 1981.

[17] W. Wen and A. Lozzi, "Recognition and inspection of manufactured parts using line moments of their boundaries," *Pattern Recognit.*, vol. 26, no. 10, pp. 1461–1471, Oct. 1993.

[18] Y.-H. Lee, "Intelligent control with fuzzy technologies in the area of metal forming," *KITE*, vol. 22, no. 11, pp. 1301–1314, 1995.

[19] R. Jain, R. Kasturi, and B. G. Schunck, *Machine Vision*. New York: McGraw-Hill, 1995, pp. 295–297.

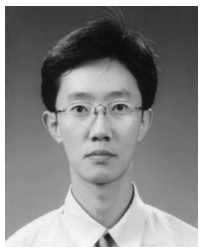

Kyung-Jin Choi received the B.S., M.S., and Ph.D. degrees in electrical engineering from Kyunghee University, Yongin, Korea, in 1996, 1998, and 2004, respectively.

He is currently an Associate Professor with the Department of Electronics, Systems and Information Engineering, Kangnam University, Yongin, and a Researcher with the Laser Micromachining R&D Center, Kangnam University. He is concerned with machine vision, image processing, embedded systems, and mobile robot control. His current research interest is in laser micromachining using a Nd:YAG UV laser system.

Young-Hyun Lee received the B.S. degree in electronics engineering from Sungkyunkwan University, Seoul, Korea, in 1981, and the Dipl.-Ing. degree in computer engineering and the Dr.-Ing. degree in engineering from RWTH Aachen, Aachen, Germany, in 1991 and 1995, respectively.

He is currently a Professor with the Department of Electronics, Systems and Information Engineering, Kangnam University, Yongin, Korea, where he is the Head of the Industrial Cooperation Foundation and the Chief of the Laser Micromachining R&D Center. He is concerned with fuzzy control and embedded system. His current research interest is in laser micromachining using laser systems.

Jong-Woo Moon received the B.S., M.S., and Ph.D. degrees in electrical engineering from Kyunghee University, Yongin, Korea, in 1990, 1992, and 2000, respectively.

He is currently a Professor with the Department of Electronics, Busan College of Information Technology, Busan, Korea. He is concerned with control theory, microprocessors, and their applications.

Chong-Kug Park (M'89) was born in Korea in 1945. He received the B.S. degree in physics from Seoul National University, Seoul, Korea, in 1971, and the M.S. and Ph.D. degrees in electrical engineering from Yonsei University, Seoul, in 1975 and 1979, respectively.

From 1987 to 1988, he was a Visiting Professor at Oregon State University. Corvallis. From 2001 to 2004, he was the Dean of the College of Engineering, College of Electronics and Information, Graduate School of Information and Communication, Kyunghee University, Seoul, where he is currently a Professor. His research interests are in robotics, mechatronics, fuzzy logic, and neural networks.

Prof. Park is a Fellow of the Society of Instrument and Control Engineers of Japan and the Institute of Control, Automation and Systems Engineers (ICASE, Korea). He was the President of the Korea Fuzzy Logic and Intelligent Systems (KFIS) Society from 1998 to 1999 and the Vice President of the Institute of Electronic Engineers in Korea (IEEK) from 2003 to 2005. He is currently the President of ICASE. He was a recipient of the Academic Achievement Award from the Korea Institute of Electrical Engineers in 1979 and Distinguished Service Awards from IEEK and KFIS in 1996 and 2000, respectively.

Fumio Harashima (M'75–SM'81–F'88) was born in Tokyo, Japan, in 1940. He received the B.S., M.S., and Ph.D. degrees from the University of Tokyo, Tokyo, in 1962, 1964, and 1967, respectively, all in electrical engineering.

He was with the Institute of Industrial Science, University of Tokyo, as an Associate Professor in 1967, a Professor from 1980 to 1998, and the Director from 1995 to 1997. He was the President of Tokyo Metropolitan Institute of Technology, Tokyo, from April 1998 to March 2002. He was a Visiting Professor with the Korea Advanced Institute of Science and Technology, Daejon, Korea, in 2002–2003. He has been an elected President of Tokyo Denki University since June 15, 2004 (with four-year term), where he is also a Professor. He has been a Professor Emeritus with the University of Tokyo since April 2000. His research interests are in power electronics, mechatronics, and robotics. He is the coauthor of four books and has published more than 1000 technical papers in the above areas.

Dr. Harashima has been active in various academic societies such as the Institute of Electrical Engineers (IEE) of Japan, the Society of Instrument and Control Engineers (SICE) of Japan, and the Robotics Society of Japan. He is a Fellow of SICE. He served as President of the IEEE Industrial Electronics Society (IES) in 1986–1987 and as Secretary in 1990. He was also a member of the IEEE N&A Committee in 1991–1992 and the IEEE Fellows Committee in 1991–1993. He served as the Founding Editor-in-Chief of the IEEE/ASME TRANSACTIONS ON MECHATRONICS in 1995. He is currently an Associate Editor of the IEEE TRANSACTIONS ON INDUSTRIAL ELECTRONICS. He served as President of the IEE Japan in 2001–2002. He was a recipient of a number of awards, including the 1978 SICE Best Paper Award, the 1983 IEE of Japan Best Paper Award, the 1984 IEEE/IES Anthony J. Hornfeck Award, the 1988 IEEE/IES Eugene Mittelmann Award, and the IEEE Third Millennium Medal. He was also awarded the "Officier dans l'Ordre des Palmes Academiques" from the Republic of France.